

Modified commercial UV curable elastomers for passive 4D printing

Hardik Hingorani, Yuan-Fang Zhang, Biao Zhang, Ahmad Serjouei & Qi Ge

To cite this article: Hardik Hingorani, Yuan-Fang Zhang, Biao Zhang, Ahmad Serjouei & Qi Ge (2019): Modified commercial UV curable elastomers for passive 4D printing, International Journal of Smart and Nano Materials, DOI: [10.1080/19475411.2019.1591540](https://doi.org/10.1080/19475411.2019.1591540)

To link to this article: <https://doi.org/10.1080/19475411.2019.1591540>



© 2019 The Author(s). Published by Informa UK Limited, trading as Taylor & Francis Group.



Published online: 20 Mar 2019.



Submit your article to this journal [↗](#)



Article views: 352



View Crossmark data [↗](#)

Modified commercial UV curable elastomers for passive 4D printing

Hardik Hingorani^a, Yuan-Fang Zhang^a, Biao Zhang^a, Ahmad Serjouei^a and Qi Ge^{a,b}

^aDigital Manufacturing and Design Centre, Singapore University of Technology and Design, Singapore;

^bScience and Math Cluster, Singapore University of Technology and Design, Singapore

ABSTRACT

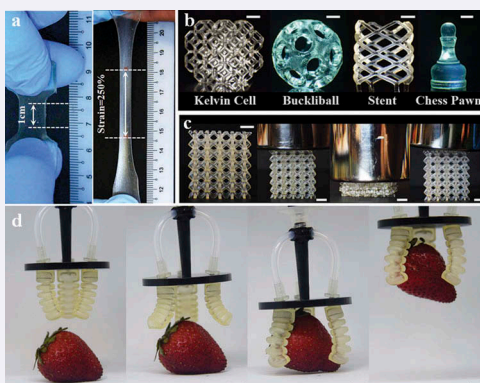
Conventional 4D printing technologies are realized by combining 3D printing with soft active materials such as shape memory polymers (SMPs) and hydrogels. However, the intrinsic material property limitations make the SMP or hydrogel-based 4D printing unsuitable to fabricate the actuators that need to exhibit fast-response, reversible actuations. Instead, pneumatic actuations have been widely adopted by the soft robotics community to achieve fast-response, reversible actuations, and many efforts have been made to apply the pneumatic actuation to 3D printed structures to realize passive 4D printing with fast-response, reversible actuation. However, the 3D printing of soft actuators/robots heavily relies on the commercially available UV curable elastomers the break strains of which are not sufficient for certain applications which require larger elastic deformation. In this paper, we present two simple approaches to tune the mechanical properties such as stretchability, stiffness, and durability of the commercially available UV curable elastomers by adding: (i) mono-acrylate based linear chain builder; (ii) urethane diacrylate-based crosslinker. Material property characterizations have been performed to investigate the effects of adding the two additives on the stretchability, stiffness, mechanical repeatability as well as viscosity. Demonstrations of fully printed robotic finger, grippers, and highly deformable 3D lattice structure are also presented.

ARTICLE HISTORY

Received 7 October 2018
Accepted 29 January 2019

KEYWORDS

4D printing; elastomer; highly stretchable; soft robots



CONTACT Qi Ge  ge_qi@sutd.edu.sg  Digital Manufacturing and Design Centre, Singapore University of Technology and Design, Singapore 487372

© 2019 The Author(s). Published by Informa UK Limited, trading as Taylor & Francis Group.

This is an Open Access article distributed under the terms of the Creative Commons Attribution License (<http://creativecommons.org/licenses/by/4.0/>), which permits unrestricted use, distribution, and reproduction in any medium, provided the original work is properly cited.

1. Introduction

Recently, four-dimensional (4D) printing as an emerging technology has gained great attention due to its capability of enabling three-dimensionally (3D) printed structures to change shape over time upon environmental stimuli such as temperature [1–4], water [5–11] and light [12,13]. Conventionally, 4D printing can be realized through 3D printing complex structures using soft active materials (SAM) such as shape memory polymers (SMPs) and hydrogels. SMPs that exhibit the shape memory effect due to the glass transition between the glassy and the rubbery states have been applied to realize 4D printing. Examples include printed active composites [3], active origami [4], 4D printed box with sequential folding [14], high-resolution multimaterial 4D printing [15] and others [16–19]. However, the fact that it always requires the application of an external load after the completion of a shape memory cycle makes SMP-based 4D printing unsuitable to applications that require reversible actuation. In contrast, hydrogel-based 4D printing enables reversible actuation as the loosely crosslinked hydrogel network swells after absorbing solvent and shrinks when the solvent evaporates. Nevertheless, the physical diffusion processes of solvent absorption and evaporation usually take more than minutes and even hours [9,10], which renders hydrogel-based 4D printing not practical in applications that require fast actuation rates.

Pneumatic actuations that are realized by applying pressurized air to inflate soft elastic actuator cavity have been widely adopted by the soft robotics community to achieve fast-response, reversible actuations [20–23]. Recently, many efforts have been made to apply the pneumatic actuation to 3D printed structures to realize fully 3D printed soft actuators/robots which can also be referred to as passive 4D printing with fast-response, reversible actuation [24–28]. However, the 3D printing of soft actuators/robots heavily relied on the commercially available UV curable elastomers such as Stratasys TangoPlus, Formlab Flexible and Spot-A Elastic [24], whose failure strains are less than 120% and not sufficient for certain applications which require larger elastic deformation. In addition, for the researchers with mechanical engineering background, it is challenging to tune the mechanical performance of the commercially available UV curable elastomers by adding other chemical ingredients.

In this paper, we present two simple approaches to tune the mechanical properties such as stretchability, stiffness, and repeatability of the commercially available UV curable elastomers by adding two chemical additives: (i) mono-acrylate based linear chain builder; (ii) urethane diacrylate-based crosslinker. After adding the chemical additives, the stretchability of elastomers can be significantly improved, which greatly enhances the capability of elastomers to realize the pneumatic actuation based passive 4D printing. We use TangoPlus as the sample elastomer to study the effects of adding two chemical additives on the mechanical properties. Without losing generality, the presented approaches can also be applied to other commercially available elastomers.

2. Material and process

2.1 Materials preparation

The sample commercial UV curable elastomer, TangoPlus, was purchased from Stratasys (MN, USA). Although the detailed chemical structure of TangoPlus is not revealed, based

on the safety data sheet, the approximate acrylate-based chemical structure is presented in Figure 1(a). Epoxy Aliphatic Acrylate (EAA) is chosen as the mono-acrylate linear chain builder, and Aliphatic Urethane-based Diacrylate (AUD) is chosen as the urethane diacrylate-based crosslinker. Both EAA (tradename: Ebecryl 113) and AUD (tradename: Ebecryl 8413) were donated by Allnex (Malaysia). The detailed chemical structures of EAA and AUD are also presented in Figure 1(a). To modify the mechanical performance of TangoPlus, the EAA/AUD with a certain weight percentage was added to the TangoPlus resin. For 100% AUD and 100% EAA as control samples, 2% (w/w) TPO was used as the photo-initiator. The mixtures were stirred on a magnetic stirrer for about 2

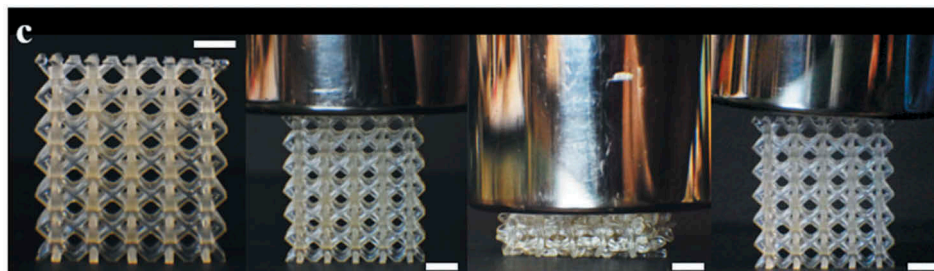
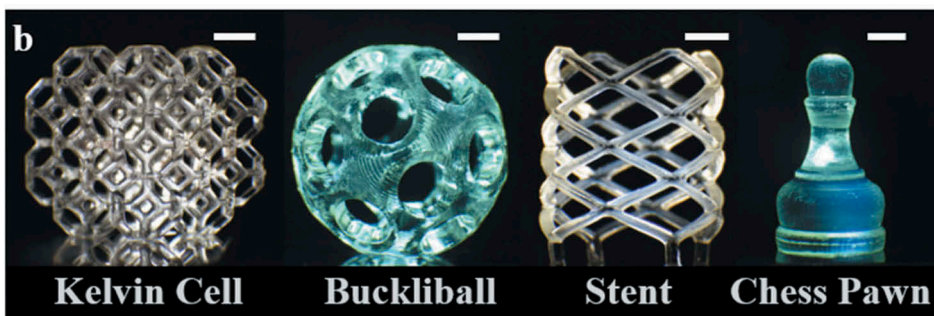
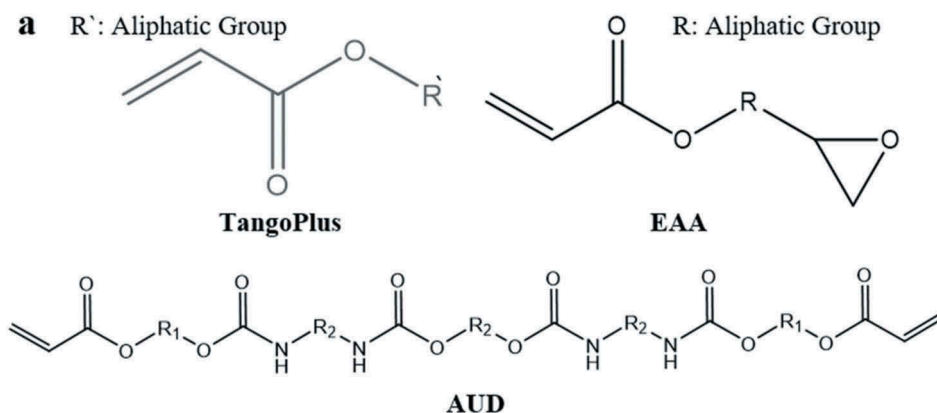


Figure 1. Modified TangoPlus. (a) Detailed chemical structures of TangoPlus, EAA, and AUD. (b) Demonstration of high-resolution structures printed with a modified TangoPlus polymer solution (TangoPlus/EAA = 6:4). (c) Demonstration of the high elastic deformability of a printed lattice structure printed with a modified TangoPlus polymer solution (TangoPlus:AUD = 8:2). The scale bars are 5 mm.

h and then de-gassed. For the Tango-AUD system, due to the high viscosity of AUD, the mixing was carried out in an oil bath at 40°C.

2.2 Sample printing

The mechanical testing samples and 3D structures were printed on a self-built digital processing based high-resolution 3D printing system [15]. Briefly, the 3D printing system consists of a CEL5500 LED light engine purchased from Digital Light Innovation (Austin, Texas, USA) with 405 nm wavelength near UV light as the digital micro-display, and a translation stage (LTS300) with 0.1 μm achievable incremental movement and 2 μm backlash purchased from Thorlabs (Newton, New Jersey, USA) as elevator. The projection area is about 3.2 cm \times 2.4 cm resulting in a pixel size of \sim 30 μm \times 30 μm . The printed layer thickness was set as 50 μm . Figure 1(b) presents the printed high-resolution elastomeric structures. Figure 1(c) demonstrates the high elastic deformability of a printed lattice structure.

3. Material property characterization

3.1 Uniaxial tensile test

Uniaxial tensile tests were performed to investigate the effects of adding EAA/AUD on the mechanical performance of the modified TangoPlus. All the tests were conducted on an MTS uniaxial tensile testing machine (Criterion Model 43, MN USA) under 10 mm/min strain rate. All the samples with 25 mm \times 10 mm \times 1 mm dimensions were 3D printed. The digital-image-correlation (DIC) system was used to measure the strain.

Figure 2(a) presents the stress–strain behaviors of the modified TangoPlus with various weight percentages ranging from 20% to 80%. In addition, the stress–strain behaviors of pure TangoPlus and EAA are also plotted for comparison. Overall, the increase in the weight fraction of EAA improves the stretchability of the modified TangoPlus but also results in the decrease in stiffness. Figure 2(b) summarizes the effect of adding EAA with different weight fractions on the mechanical performance on the modified TangoPlus. Increasing the weight fraction of EAA from 0 to 100 wt.% results in the increase in the break strain from 110% to 520% and the decrease in modulus from 0.7 MPa to 0.1 MPa. To demonstrate the improvement, we compare the stretchability of a dog-bone sample printed using pure TangoPlus with that of the one printed using the modified TangoPlus after adding EAA (TangoPlus:EAA = 6:4). As shown in Figure 2(c), the stretchability is improved by 83% after adding 40 wt.% EAA. The illustration in Figure 2(d) explains the mechanism. During UV triggered photopolymerization, the EAA monomers form linear chains that increase the lengths of the linear chains in the original network of TangoPlus. The length-increase in the linear chains greatly improve the stretchability of the network system. However, the addition of the mono-acrylate based EAA reduces the concentration of crosslinkers in the system, leading to lower stiffness.

Certain applications require the enhancements in both stretchability and stiffness. To meet this requirement, the crosslinkers that improve the stretchability of the polymer network are needed. The previous study shows that urethane diacrylate-based crosslinker, AUD, has the ability to enhance both stretchability and stiffness due to the

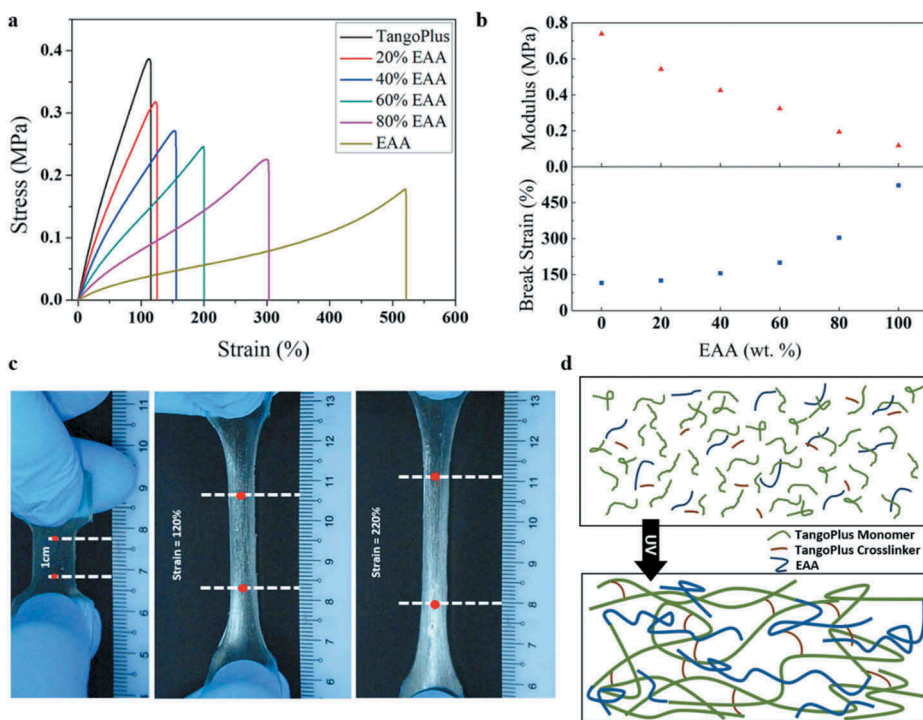


Figure 2. TangoPlus modified by EAA. (a) Stress–strain behaviors of the samples made of the modified TangoPlus with different weight fractions of EAA. (b) The effect of weight fractions of EAA on the mechanical performance of modified TangoPlus. (c) The demonstration shows that the stretchability is increased by 83% after adding 40 wt. % EAA. (d) Illustration explains the mechanism of adding EAA to improve the stretchability.

presence of hydrogen bonds between hard domains of AUD [24]. Therefore, we performed uniaxial tensile tests to investigate the effects of adding AUD on the mechanical improvement of the modified TangoPlus. Figure 3(a) presents the stress–strain behaviors of the modified TangoPlus with various weight percentages of AUD ranging from 20% to 80% along with the stress–strain behaviors of pure TangoPlus and pure AUD for comparison. The stretchability of the modified TangoPlus is greatly improved with the addition of AUD. Besides, the apparent nonlinear stress–strain behavior is observed after adding AUD with more than 40 wt. %. Figure 3(b) summarizes the effect of adding AUD with different weight fractions on the mechanical performance on the modified TangoPlus. The stretchability increases from 100% to more than 400% with the increase in the weight fraction of AUD from 0% to 100%, and the modulus also increases from 0.7 MPa to more than 8 MPa. Based on the requirements from specific applications, users can add moderate AUD into TangoPlus to achieve desired stretchability and stiffness. To demonstrate the improvement, we compare the stretchability of a dog-bone sample printed using pure TangoPlus with that of the one printed using the modified TangoPlus after adding AUD (TangoPlus:AUD = 8:2). As shown in Figure 3(c), the stretchability is improved by 108% after adding 20 wt.% AUD. The illustration in Figure 3(d) depicts the mechanism. Diacrylate based AUD works as crosslinker, and the increase in AUD results

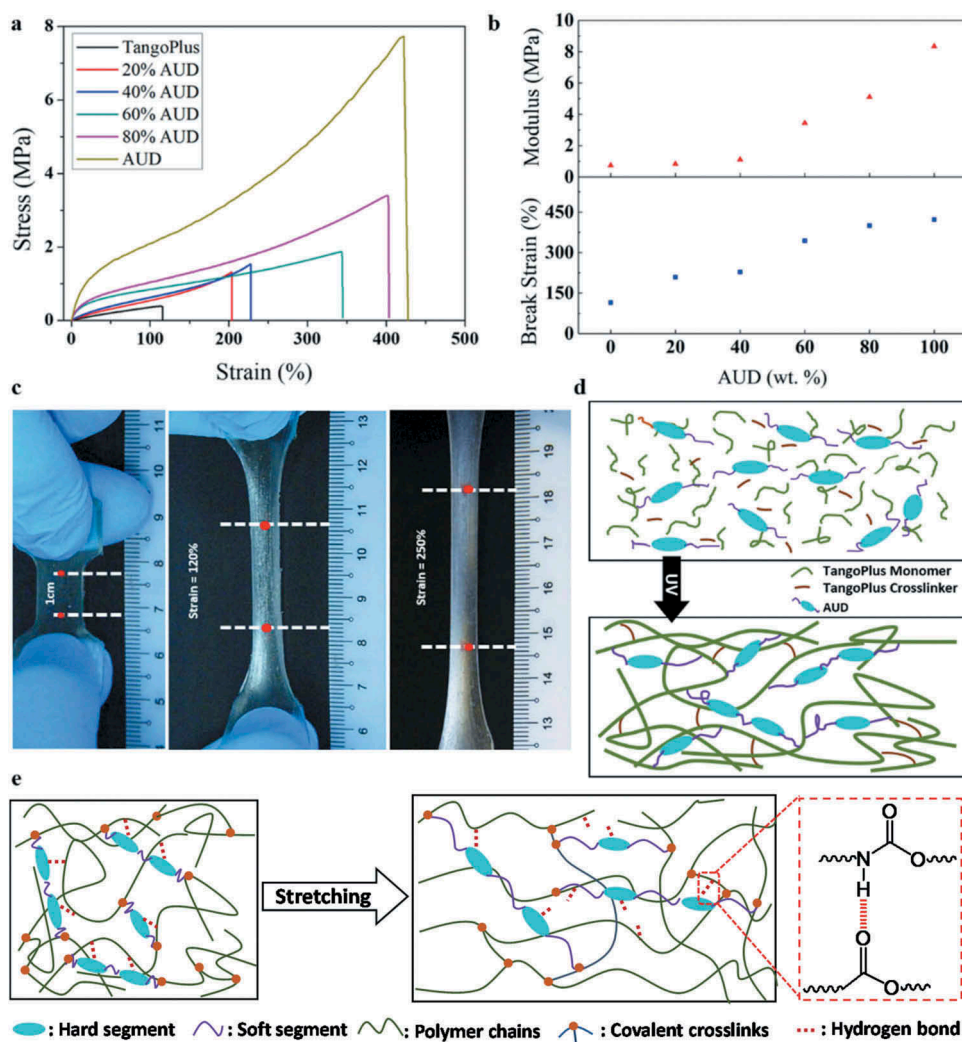


Figure 3. TangoPlus modified by AUD. (a) Stress–strain behaviors of the samples made of modified TangoPlus with different weight fractions of AUD. (b) The effect of weight fractions of AUD on the mechanical performance of modified TangoPlus. (c) The demonstration shows that the stretchability is increased by 108% after adding 20 wt. % AUD. (d) Illustration explains the mechanism of adding AUD to enhance the stiffness. (e) Illustration explains the mechanism of adding AUD to enhance the stretchability.

in high crosslinking density of the modified network, therefore, higher stiffness. In addition, the increase in the AUD also leads to an increase in the hydrogen bonds between hard domains of AUD [29–31]. As shown in Figure 3(e), upon a mechanical loading, the breakage of hydrogen bonds dissipates energy and therefore results in the higher stretchability of the elastomer system [32].

3.2 Mechanical cyclic tests

In applications such as soft robotics, the constituent materials are required to have good mechanical durability to allow repeated actuation. Therefore, we performed the loading-unloading cyclic tests to investigate the improvement on the mechanical durability of the modified TangoPlus. The tests were conducted on a fatigue tester (Electroforce 3200, TA Instrument, MN, USA). The printed samples with dimensions of 15 mm × 5 mm × 1 mm were subjected to cyclic loading in between 20% and 100% strain. Figure 4(a–c) compare cyclic testing results of the samples made of pure TangoPlus, TangoPlus modified by EAA (TangoPlus:EAA = 7:3) and TangoPlus modified by AUD (TangoPlus:AUD = 7:3). The pure TangoPlus sample fails after 140 loading-unloading cycles (Figure 4(a)). The numbers of the loading-unloading cycles are increased to 400 and 2000 after adding 30 wt.% of EAA and AUD, respectively. Figure 4(d–f) present the stress–strain behaviors during the cyclic tests for TangoPlus, TangoPlus modified by EAA, and TangoPlus modified by AUD. All the tests exhibit the hysteresis loops indicating the energy dissipation during the loading-unloading cycles. The energy dissipations on pure TangoPlus and TangoPlus modified by EAA can be attributed to the permanent damage on the covalent bonds, while the energy dissipation on TangoPlus modified by AUD mainly comes from the breakage on the reversible hydrogen bonds which make it able to sustain 2000 cycles.

3.3 Rheological test

Viscosity of the polymer solutions is one of the key material parameters for the DLP-based 3D printing. After the completion of one-layer printing, the printing platform moves up (or down) to the position for the next layer. The motion of the printing platform disturbs the surface of the polymer solution, and the printer needs to wait for

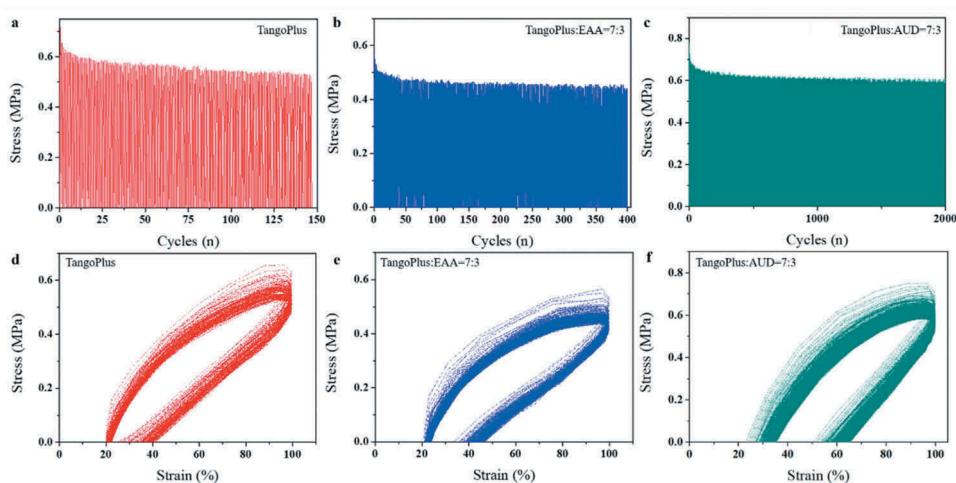


Figure 4. Loading-unloading cyclic tests. (a–c) Stress variations vs cycling numbers for the samples made of TangoPlus, TangoPlus modified by EAA, and TangoPlus modified by AUD, respectively. (d–f) Stress–strain behaviors during the loading-unloading cycles for the samples made of TangoPlus, TangoPlus modified by EAA, and TangoPlus modified by AUD, respectively.

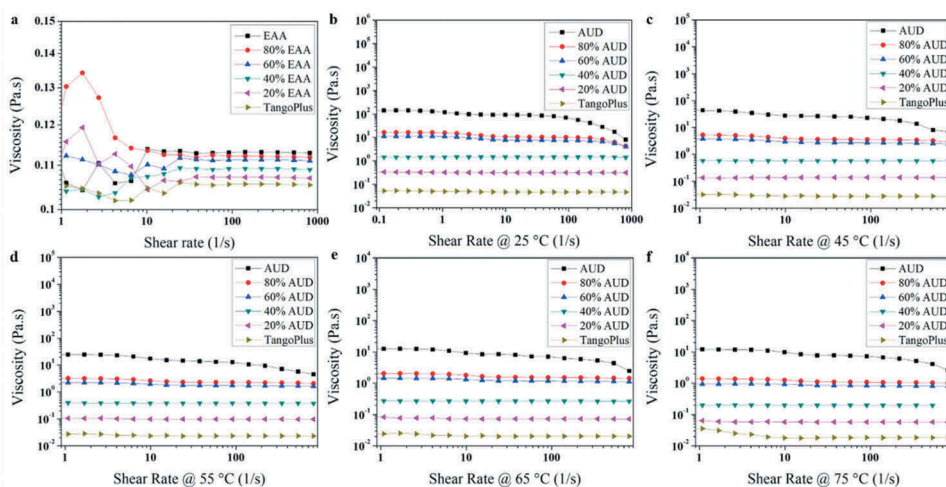


Figure 5. Rheological tests of the modified TangoPlus solutions. (a) Rheological tests at 25°C of the modified TangoPlus solutions by adding EAA. (b)–(f) Rheological tests of the modified TangoPlus solutions by adding AUD at 25°C 45°C, 55°C, 65°C and 75°C, respectively.

the disturbance to cease. Higher viscosity requires a longer waiting time. Therefore, we performed the rheological tests to investigate the effect of adding EAA/AUD on the viscosity of the modified TangoPlus solution. The rheological tests were conducted on a Discovery Hybrid Rheometer (DHR2, TA instruments Inc., UK) with an aluminum plate geometry (diameter 40 mm). [Figure 5\(a\)](#) shows that for the modified TangoPlus, by adding EAA, the viscosity is independent of shear rate in the range 10 s^{-1} to 1000 s^{-1} . The addition of EAA slightly increases the viscosity of the modified TangoPlus solution, but overall viscosity is about 0.11 Pa·s which is low enough for 3D printing. For the AUD modified TangoPlus, as shown in [Figure 5\(b\)](#), the viscosity is independent of shear rate in the range 0.1 s^{-1} to 1000 s^{-1} , and the viscosity of the modified TangoPlus increases remarkably from $\sim 0.1 \text{ Pa}\cdot\text{s}$ to $\sim 100 \text{ Pa}\cdot\text{s}$ on increasing the weight fraction of AUD from 0 wt.% to 100 wt. %. Generally, when the viscosity is higher than 1 Pa·s, the polymer solution is not suitable for the DLP-based 3D printing as the waiting time for each layer is more than 1 min. Heating is an efficient way to reduce the viscosity of polymer solution. Therefore, [Figure 5\(b–f\)](#) present the rheological testing results of modified TangoPlus by adding AUD at 45°C, 55°C, 65°C and 75°C, respectively. Heating significantly decreases the viscosity of the polymer solutions. At 75°C, the viscosity of the modified TangoPlus with 80 wt.% is also reduced to 1 Pa·s which is an acceptable viscosity of DLP-based 3D printing.

4. Demonstration of passive 4D printing

To demonstrate the high stretchability of modified TangoPlus solutions, we printed a millimeter-scale (5 mm in width) pneumatic finger actuator using the modified TangoPlus by adding 30 wt. % of EAA. As shown in [Figure 6\(a\)](#), the initially straight finger actuator bends after applying the pressurized air into the cavity of the actuator body. We

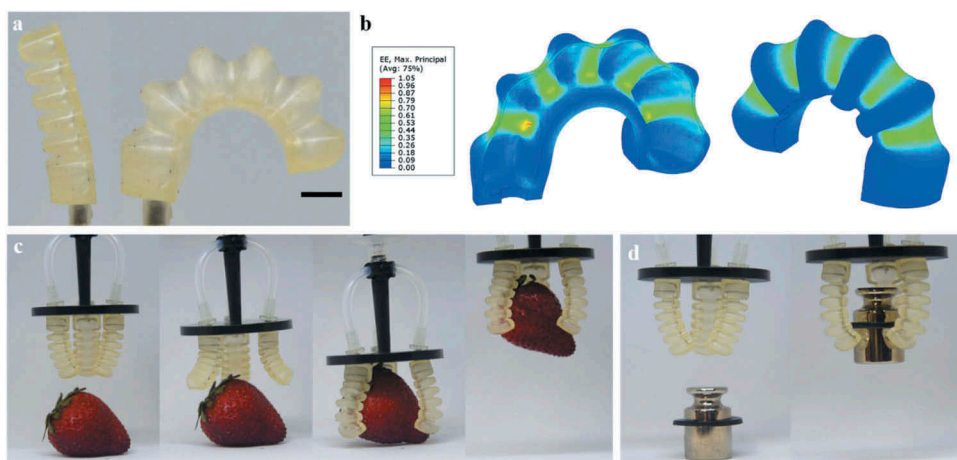


Figure 6. Demonstration of the fully printed millimeter-scale soft actuator. (a) The actuator at initial straight configuration and inflated bent configuration. The scale bar is 5 mm. (b) Strain contour of the finger actuator under the largest bending angle. (c) A mini soft gripper that grabs and lifts a strawberry. (d) A mini soft gripper that grabs and lifts a 50 g weight.

conducted Finite Element (FE) simulations to investigate the local deformations on the pneumatic finger actuator. The FE simulations were performed on a commercial FE software ABAQUS (V6.14, Dassault Systèmes Simulia Corp., USA). The Mooney-Rivlin model was used to describe the stress–strain behavior of the Modified TangoPlus by EAA. The strain energy potential of the Mooney-Rivlin model is given by $U = C_{10} (\bar{I}_1 - 3) + C_{01} (\bar{I}_2 - 3) + 1/D_1 (J-1)^2$, where U is the strain energy density, C_{10} , C_{01} and D_1 are material parameters. By fitting the stress–strain curve, we obtain $C_{10} = 0.089$ MPa, $C_{01} = -0.021$ MPa. Figure 6(b) presents the strain contour on the finger actuator under the largest bending angle. The simulation reveals that the local maximum strain is about 105%. After assembling three printed pneumatic finger actuators, we built a mini soft gripper which easily conforms to the surface geometry of a strawberry and lifts the 15 g fruit (Figure 6(c)) with ease and the maximum load that the gripper could bear was found to be 50 g (Figure 6(d)). It should be noted that the traditional molding-casting method has been widely used in the fabrication of pneumatic soft actuators and robots, but it is not suitable at this millimeter-scale fabrication.

Not only do the modified TangoPlus by AUD sustain large elastic deformation, but also maintain good mechanical repeatability of more than 1000 times loading/unloading cycles. Based on this, we fabricated a highly stretchable and electric conductive 3D lattice structure which can be potentially used as a flexible electronic device. As shown in Figure 7(a), we first printed out a lattice structure using TangoPlus modified by 20 wt. % AUD. Then, we coated a thin conductive hydrogel layer by immersing the lattice structure into a conductive hydrogel solution which was prepared by mixing acrylamide as the monomer, poly (ethylene glycol) diacrylate (PEGDA) as the crosslinker, and 2,4,6 – trimethylbenzoyl – diphenylphosphine oxide as the photoinitiator into 80 wt. % water [33]. A small amount of sodium chloride was added to make the hydrogel solution conductive. UV irradiation cured the hydrogel layer. Figure 7(b) shows that the conductive hydrogel coated 3D lattice

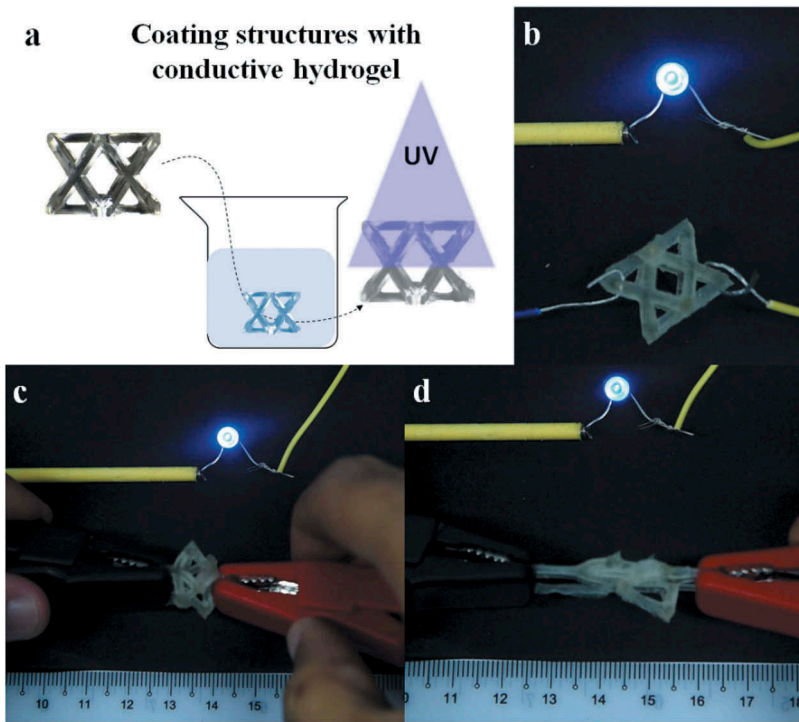


Figure 7. Highly stretchable electric conductive 3D structure. (a) Coating process. (b)–(d) The conductive hydrogel coated 3D lattice structure shows good conductivity under no deformation, compression, and stretching, respectively.

structure has good conductivity. The 3D lattice structure keeps good conductivity under compression (Figure 7(c)) and stretching (Figure 7(d)).

5. Conclusion

In this paper, we present two simple approaches to tune the mechanical properties such as stretchability, stiffness, and durability of the commercially available UV curable elastomers by adding: (i) mono-acrylate based linear chain builder; (ii) urethane diacrylate-based crosslinker. Material property characterizations have been performed to investigate the effects of adding the two additives on the stretchability, stiffness, mechanical durability as well as viscosity. Demonstrations of fully printed robotic finger, grippers, and highly deformable 3D lattice structure are also presented.

Acknowledgments

We acknowledge support from the Agency for Science, Technology and Research (A*STAR) Public Sector Funding (PSF) (Project number 1521200086). Q.G. acknowledges SUTD Start-up Research Grant.

Disclosure statement

No potential conflict of interest was reported by the authors.

Funding

This work was supported by the SUTD Startup Research Grant; Agency for Science, Technology and Research (A*STAR) Public Sector Funding (PSF) [1521200086].

References

- [1] A. Lendlein and S. Kelch, *Shape-memory polymers*, *Angew. Chem. Weinheim. Bergstr. Ger.* 41 (2002), pp. 2034–2057. doi:10.1002/1521-3773(20020617)41:12<2034::AID-ANIE2034>3.0.CO;2-M.
- [2] A. Lendlein and S. Kelch, *Shape-memory polymers as stimuli-sensitive implant materials*, *Clin. Hemorheol. Microcirc.* 32 (2005), pp. 105–116.
- [3] Q. Ge, H.J. Qi, and M.L. Dunn, *Active materials by four-dimension printing*, *Appl. Phys. Lett.* 103 (2013), pp. 131901. doi:10.1063/1.4819837.
- [4] Q. Ge, C.K. Dunn, H.J. Qi, and M.L. Dunn, *Active origami by 4D printing*, *Smart. Mater. Struct.* 23 (2014), pp. 094007. doi:10.1088/0964-1726/23/9/094007.
- [5] S. Tibbits, *The emergence of “4D printing”, TED conference, 2013*, Long Beach, California, U.S.A.
- [6] M. Jamal, S.S. Kadam, R. Xiao, F. Jivan, T.M. Onn, R. Fernandes, T.D. Nguyen, and D.H. Gracias, *Bio-origami hydrogel scaffolds composed of photocrosslinked PEG bilayers*, *Adv. Healthc. Mater.* 2 (2013), pp. 1142–1150. doi:10.1002/adhm.201200458.
- [7] E. Palleau, D. Morales, M.D. Dickey, and O.D. Velev, *Reversible patterning and actuation of hydrogels by electrically assisted ionoprinting*, *Nat. Commun.* 4 (2013), p. 2257. doi:10.1038/ncomms3257.
- [8] L. Ionov, *Biomimetic hydrogel-based actuating systems*, *Adv. Funct. Mater.* 23 (2013), pp. 4555–4570. doi:10.1002/adfm.v23.36.
- [9] D. Raviv, W. Zhao, C. McKnelly, A. Papadopoulou, A. Kadambi, B. Shi, S. Hirsch, D. Dikovskiy, M. Zyracki, C. Olguin, R. Raskar, and S. Tibbits, *Active printed materials for complex self-evolving deformations*, *Sci. Rep.* 4 (2014), pp. 7422. doi:10.1038/srep07422.
- [10] A.S. Gladman, E.A. Matsumoto, R.G. Nuzzo, L. Mahadevan, and J.A. Lewis, *Biomimetic 4D printing*, *Nat. Mater.* 15 (2016), pp. 413–418. doi:10.1038/nmat4544.
- [11] M. Wehner, R.L. Truby, D.J. Fitzgerald, B. Mosadegh, G.M. Whitesides, J.A. Lewis, and R. J. Wood, *An integrated design and fabrication strategy for entirely soft, autonomous robots*, *Nature* 536 (2016), pp. 451–+. doi:10.1038/nature19100.
- [12] K.N. Long, T.F. Scott, H.J. Qi, C.N. Bowman, and M.L. Dunn, *Photomechanics of light-activated polymers*, *J. Mech. Phys. Solids* 57 (2009), pp. 1103–1121. doi:10.1016/j.jmps.2009.03.003.
- [13] J. Ryu, M. D’Amato, X.D. Cui, K.N. Long, H.J. Qi, and M.L. Dunn, *Photo-origami—Bending and folding polymers with light*, *Appl. Phys. Lett.* 100 (2012), 100.
- [14] Y. Mao, K. Yu, M.S. Isakov, J. Wu, M.L. Dunn, and H.J. Qi, *Sequential self-folding structures by 3D printed digital shape memory polymers*, *Sci. Rep.* 5 (2015), pp. 13616. doi:10.1038/srep13616.
- [15] Q. Ge, A.H. Sakhaei, H. Lee, C.K. Dunn, N.X. Fang, and M.L. Dunn, *Multimaterial 4D printing with tailorable shape memory polymers*, *Sci. Rep.* 6 (2016), pp. 31110. doi:10.1038/srep31110.
- [16] M. Zarek, M. Layani, I. Cooperstein, E. Sachyani, D. Cohn, and S. Magdassi, *3D printing of shape memory polymers for flexible electronic devices*, *Adv. Mater.* 28 (2016), pp. 4449–4454. doi:10.1002/adma.201503132.

- [17] Z. Ding, C. Yuan, X. Peng, T. Wang, H.J. Qi, and M.L. Dunn, *Direct 4D printing via active composite materials*, *Sci. Adv.* 3 (2017), pp. e1602890. doi:10.1126/sciadv.1602890.
- [18] Z. Ding, O. Weeger, H.J. Qi, and M.L. Dunn, *4D rods: 3D structures via programmable 1D composite rods*, *Mater. Des.* 137 (2017), pp. 256–265.
- [19] S. Akbari, A.H. Sakhaei, K. Kowsari, B. Yang, A. Serjouei, Y.F. Zhang, and G. Qi, *Enhanced multimaterial 4D printing with active hinges*, *Smart. Mater. Struct.* 27 (2018). doi:10.1088/1361-665X/aabe63.
- [20] R.F. Shepherd, F. Ilievski, W. Choi, S.A. Morin, A.A. Stokes, A.D. Mazzeo, X. Chen, M. Wang, and G.M. Whitesides, *Multigait soft robot*, *P. Natl. Acad. Sci. USA* 108 (2011), pp. 20400–20403. doi:10.1073/pnas.1116564108.
- [21] B. Mosadegh, P. Polygerinos, C. Keplinger, S. Wennstedt, R.F. Shepherd, U. Gupta, J. Shim, K. Bertoldi, C.J. Walsh, and G.M. Whitesides, *Pneumatic networks for soft robotics that actuate rapidly*, *Adv. Funct. Mater.* 24 (2014), pp. 2163–2170. doi:10.1002/adfm.v24.15.
- [22] M.T. Tolley, R.F. Shepherd, B. Mosadegh, K.C. Galloway, M. Wehner, M. Karpelson, R.J. Wood, and G.M. Whitesides, *A resilient, untethered soft robot*, *Soft Robot.* 1 (2014), pp. 213–223. doi:10.1089/soro.2014.0008.
- [23] D. Rus and M.T. Tolley, *Design, fabrication and control of soft robots*, *Nature* 521 (2015), pp. 467–475. doi:10.1038/nature14543.
- [24] D.K. Patel, A.H. Sakhaei, M. Layani, B. Zhang, Q. Ge, and S. Magdassi, *Highly stretchable and UV curable elastomers for digital light processing based 3D printing*, *Adv. Mater.* 29 (2017). doi:10.1002/adma.201700681.
- [25] T.J. Wallin, J.H. Pikul, S. Bodkhe, B.N. Peele, B.C. Mac Murray, D. Therriault, B.W. McEnerney, R. P. Dillon, E.P. Giannelis, and R.F. Shepherd, *Click chemistry stereolithography for soft robots that self-heal*, *J. Mater. Chem. B* 5 (2017), pp. 6249–6255. doi:10.1039/C7TB01605K.
- [26] C.J. Thrasher, J.J. Schwartz, and A.J. Boydston, *Modular elastomer photoresins for digital light processing additive manufacturing*, *ACS Appl. Mater. Inter.* 9 (2017), pp. 39708–39716. doi:10.1021/acsami.7b13909.
- [27] L.S. Ge, L.T. Dong, D. Wang, Q. Ge, and G.Y. Gu, *A digital light processing 3D printer for fast and high-precision fabrication of soft pneumatic actuators*, *Sens. Actuators, A* 273 (2018), pp. 285–292. doi:10.1016/j.sna.2018.02.041.
- [28] Y.F. Zhang, N. Zhang, H. Hingorani, N. Ding, D. Wang, C. Yuan, B. Zhang, G. Gu, and Q. Ge, *Fast-response, stiffness-tunable soft actuator by hybrid multimaterial 3D printing*, *Adv. Funct. Mater.* (2019), pp. 1806698. doi:10.1002/adfm.201806698.
- [29] H.J. Qi and M.C. Boyce, *Stress–strain behavior of thermoplastic polyurethanes*, *Mech. Mater.* 37 (2005), pp. 817–839. doi:10.1016/j.mechmat.2004.08.001.
- [30] J. Mattia and P. Painter, *A comparison of hydrogen bonding and order in a polyurethane and poly(urethane–urea) and their blends with poly(ethylene glycol)*, *Macromolecules* 40 (2007), pp. 1546–1554. doi:10.1021/ma0626362.
- [31] J. Park, D. Tahk, C. Ahn, S.G. Im, S.J. Choi, K.Y. Suh, and S. Jeon, *Conformal phase masks made of polyurethane acrylate with optimized elastic modulus for 3D nanopatterning*, *J. Mater. Chem. C* 2 (2014), pp. 2316–2322. doi:10.1039/c3tc32194k.
- [32] J.Y. Sun, X.H. Zhao, W.R.K. Illeperuma, O. Chaudhuri, K.H. Oh, D.J. Mooney, J.J. Vlassak, and Z. G. Suo, *Highly stretchable and tough hydrogels*, *Nature* 489 (2012), pp. 133–136. doi:10.1038/nature11409.
- [33] B. Zhang, S. Li, H. Hingorani, A. Serjouei, L. Larush, A.A. Pawar, W.H. Goh, A.H. Sakhaei, M. Hashimoto, K. Kowsari, S. Magdassi, and Q. Ge, *Highly stretchable hydrogels for UV curing based high-resolution multimaterial 3D printing*, *J. Mater. Chem. B* 6 (2018), pp. 3246–3253. doi:10.1039/C8TB00673C.